Collective Dynamics of a Weakly Coupled Electrochemical Reaction on an Array

István Z. Kiss, Yumei Zhai, and John L. Hudson*

Department of Chemical Engineering, 102 Engineers' Way, University of Virginia, Charlottesville, Virginia 22904-4741

Experiments on the collective behavior and phase synchronization of weakly coupled populations of nonidentical chaotic electrochemical oscillators are described. The weak coupling has only a small effect on the local dynamics, i.e., through changes in frequency, but it has a strong influence on the collective or overall behavior. With added weak global or short-range coupling, a deviation from the law of large numbers is observed; large, irregular, and periodic mean-field oscillations occur, along with (partial) phase synchronization.

Introduction

In chemically reacting systems, the rate of reaction is often a function of both space and time. The spatial scale of variations in fluid/solid or electrochemical systems can range from nano- through micro- to macroscopic, and variations at several scales can occur simultaneously, e.g., small-scale on a catalyst surface up to the larger scale of the reactor. The degree of interaction among the reacting sites is influenced both by the local reaction rate and by the strength and range of the coupling. A number of spatiotemporal pattern types have been observed in reaction−diffusion systems[1] in which the coupling is local; in heterogeneous chemical reactions with global coupling, such as temperature control[2] or mass or heat transfer;[3−5] and in electrochemical systems, in which the coupling arises mainly through the electric field.[6] In the latter case, the coupling range depends on the cell geometry and the conductivity of the electrolyte and can be short- or long-range. The interactions can produce not only spatial patterns but also changes of the dynamics of the individual sites. A classic example of a change in local dynamics through interactions is diffusion-induced chemical turbulence in which local coupling of periodic oscillators produces chaos.[1] Global coupling can also induce turbulence.[3] In electrochemical systems, irregular behavior has been shown to occur in both simulations[7,8] and experiments[9,10] through the coupling of periodic sites.

The focus of the present paper is on coupled oscillators in which the coupling is weak, so that there are only small quantitative effects, but no qualitative effects, on the local dynamics produced by the coupling. Nevertheless, these small effects can produce significant changes in the collective, or overall, behavior of the system. In chemically reacting systems, this spatially averaged reaction rate is often the quantity of interest because it gives the overall conversion in the reactor. The collective behavior of a reaction system is then characterized by the overall time-dependent rate of reaction.

We consider here globally coupled chaotic chemical oscillators. The main features of the collective behavior of locally and globally coupled chaotic elements in mean-field-type models of both maps and ordinary differential equations have been explored.[11,12] Without coupling, the variance of the mean field (which corresponds to the spatial average) must vary with N as $1/N$ according to the law of large numbers. Reaction systems usually contain very large numbers of reaction sites; because the variance goes to zero with large numbers, such systems will operate at steady state. In weakly coupled systems, however, simulations have shown that the law of large numbers is violated because of emerging small coherence among the oscillators.[12−16] Nontrivial collective behavior can also occur, i.e., at low coupling strengths, the behavior of the individual oscillators remains chaotic but that of the ensemble can be more regular,[11,12,14−20] even periodic.[19] Some recent simulations have shown that synchronization of the phases of the chaotic oscillators[21] is important in the development of the collective motion.[18,22,23]

In this paper, we report the results of experiments on arrays of weakly coupled electrochemical oscillators. We use an array of 64 electrodes operated in the chaotic region. The properties of the individual oscillators, notably their frequencies, vary somewhat because of heterogeneities; such heterogeneities occur naturally in experimental systems, and those here are due to variations in the surface properties of the electrodes. Although the number of reacting sites is much smaller than the number of active sites on distributed reacting surfaces, it is large enough for statistical information to be extracted and collective effects to be seen. (A brief account of some of the aspects of the collective effects can be found in a recently published letter.[24]) The reaction is the electrodissolution of Ni in sulfuric acid; the rate of the electrochemical reaction is proportional to the current, which can be measured at each electrode to obtain local as well as overall rates of reaction. Some diagnostic tools involving tests for the law of large numbers and measures of phase synchronization are used to characterize changes in dynamics with increasing coupling strengths. Coupling among the elements is added either with resistors, which produce a global coupling through changes in the potential drop across the electrode double layer, or with stirring, which changes the concentrations of chemical species at the electrode surface. The design of the resistors[9,25] enables global coupling of the electrodes to be effected without changing other parameters in the system. The coupling

* Corresponding author. E-mail: hudson@virginia.edu. Telephone: 434 924 6275. Fax: 434 982 2658.

10.1021/ie0110235 CCC: $22.00
Published on Web 06/25/2002

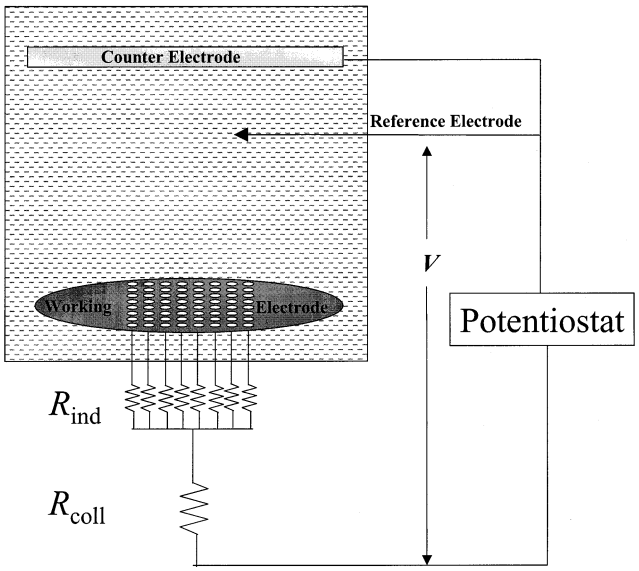

Figure 1. Schematic of the experimental setup.

effect of stirring in reactive systems can impose a global coupling through the bulk solution[3,5] and/or short-range coupling through transport among sites; we analyze the collective behavior without and with added stirring and show that, in this electrochemical system, the short-range effect is more important. We show that the weak interactions imposed on the system, either through resistive global coupling or through stirring, can have a significant effect on the collective dynamics.

Experimental Section

A schematic of the experimental apparatus is shown in Figure 1. A standard electrochemical cell consisting of a nickel working electrode array (64 1-mm-diameter electrodes in an 8 × 8 geometry), a $Hg/Hg_2SO_4/K_2SO_4$ reference electrode, and a platinum mesh counter electrode was used. The array can be thought of as a population of oscillators or as a discrete approximation of a single continuous surface when the scale of the coupling space is greater than the size of the elements and the spacing among them.[26] The potentials of all of the electrodes in the array were held at the same value (V = 1.310 V) with a potentiostat (EG&G Princeton Applied Research, model 273). Two different arrays, with 1- and 2-mm spacings between the electrodes, were used; most experiments were performed with the array having smaller spacing, and the array with larger spacing was used only for experiments on the effect of stirring. For studies on smaller arrays, sections of the 64-electrode array were used; these configurations were 1 element, 2 elements (neighbors), 4 elements (2 × 2 geometry), 16 elements (4 × 4), 36 elements (6 × 6), 49 elements (7 × 7), and 64 elements (8 × 8). The working electrodes were embedded in epoxy, and reaction took place only at the ends. The currents of the electrodes were measured independently at a sampling rate of 100 Hz, and thus, the rate of reaction as a function of position and time could be obtained. Experiments were carried out in 4.5 M H_2SO_4 solution at a temperature of 11 °C.

The electrodes were connected to the potentiostat through individual parallel resistors and through one collective series resistor (see Figure 1). We employed a method of altering the strength of global coupling[9,25,27] while holding all other parameters constant, i.e., the kinetics and the parameters of the individual oscillators were not changed. The total external resistance was held constant while the fraction dedicated to individual currents, as opposed to the total current, was varied. The external resistors could be added in parallel (individually, R_{ind}) or in series (collectively, R_{coll}). A total resistance (R_{tot}) can then be defined as

$$R_{tot} = R_{coll} + \frac{R_{ind}}{N} \tag{1}$$

where N is the number of electrodes. In these experiments, $R_{tot} = 909/N\ \Omega$. The collective resistor couples the electrodes globally: the current on one electrode affects the dynamics of the other electrodes because current through any given electrode influences the potential drop on all electrodes equally. The parameter ϵ, the ratio of collective to total resistance, is a measure of the global coupling

$$\epsilon = \frac{R_{coll}}{R_{tot}} \tag{2}$$

For $\epsilon = 0$, the external resistance furnishes no additional global coupling; for $\epsilon = 1$, maximal external global coupling is achieved. Short-range coupling was added via stirring at approximately 250 rpm (revolutions per minute) with a magnetic stirrer (diameter = 8 mm, length = 39 mm) placed approximately 45 mm below the electrode.

Results

A. Dynamics of a Single Element. We start with a description of the dynamics of the reaction on a single reaction site, i.e., on a single electrode. The time series of a chaotic state of a single oscillator is shown in Figure 2a; chaos is reached via a period-doubling bifurcation sequence as the applied potential is changed.[28,29] The chaotic attractor (Figure 2b, reconstructed from the current by the use of time delays) is low-dimensional; the information dimension characterizing the complexity of the attractor is $D_1 = 2.3 \pm 0.1$.[29] The power spectrum (Figure 2a, inset) is broad, typical of chaotic systems, with a dominant peak at f = 1.270 Hz.

A better measure of the frequency of the entire system can be found from the rate of change of the phase. The instantaneous phase and amplitude are obtained with the Hilbert transform:[30,31] the temporal mean of the current is subtracted [$I(t) = i(t) - i_{mean}$], and then the Hilbert transform, $H(I)$

$$H[I(t)] = 1/\pi \int_{-\infty}^{\infty} \frac{I(\tau)}{t - \tau}\, d\tau \tag{3}$$

is calculated and plotted vs the current I (phase portrait, Figure 2c). Note that the phase points encircle the origin, but sometimes they become very close. To increase the robustness of the phase analysis, the origin was moved to the square shown in Figure 2c. Such replacement of the origin makes the definition of phase arbitrary; however, it is still capable of describing the

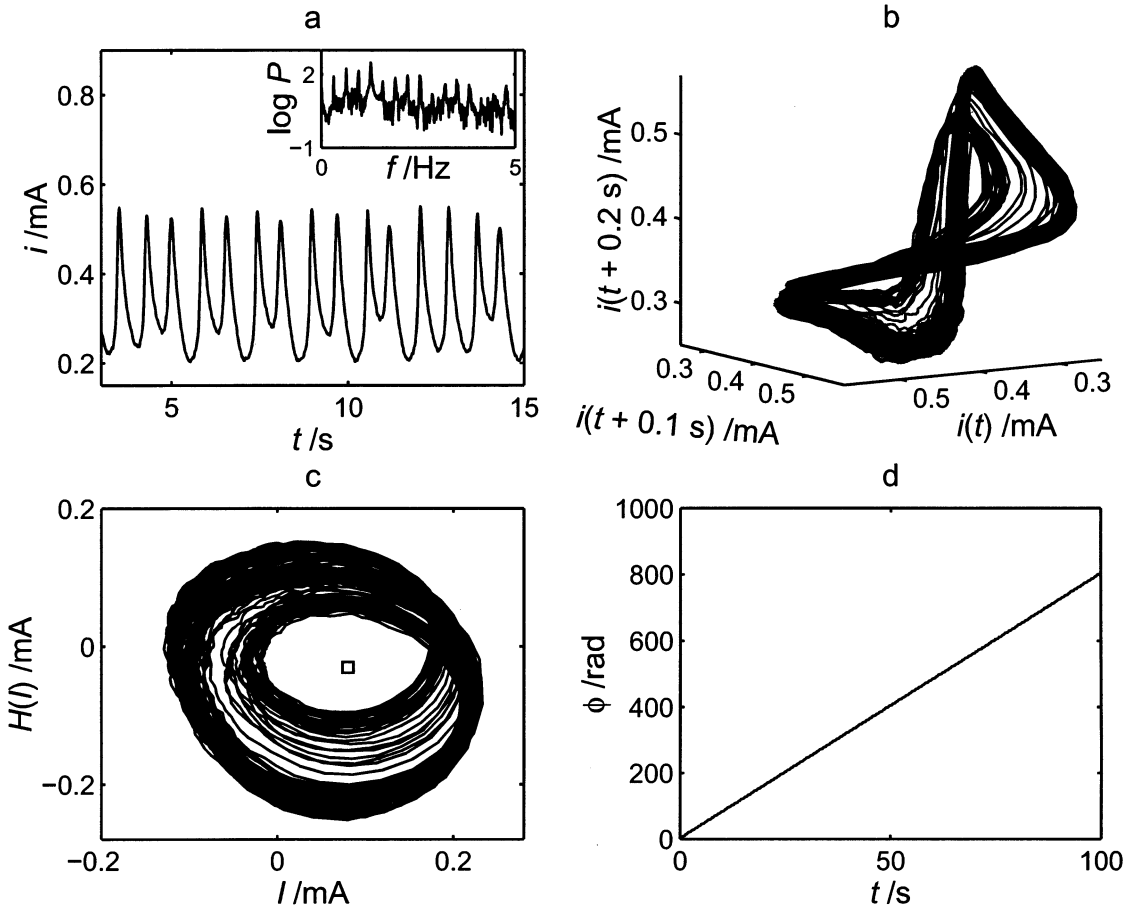

Figure 2. Chaotic dynamics of a single element. (a) Time series of current and power spectrum (inset). (b) Reconstructed attractor using time delay coordinates. (c) Phase portrait obtained with Hilbert transform. (d) Phase vs time.

dynamics of the phases in a satisfactory way.[31] Thus, at time t, the phase (ϕ) is obtained from the angle, i.e.

$$\phi(t) = \arctan\frac{H[I(t)]}{I(t)} \tag{4}$$

and the amplitude (A) gives the length

$$A(t) = \sqrt{I(t)^2 + H[I(t)]^2} \tag{5}$$

In Figure 2d, the phase is shown as a function of time. As expected, the phase is a nearly linear function of time; some small deviations from the straight line arise because of the chaotic nature of the signal. The frequency ω is calculated from the slope as

$$\omega = \frac{1}{2\pi}\left\langle\frac{\mathrm{d}\phi}{\mathrm{d}t}\right\rangle \tag{6}$$

The frequency for the single element was found to be ω = 1.275 Hz, which is close to the frequency of the dominant peak in the power spectrum.

B. Sixty-Four Elements without Added Coupling. We now turn to the array of 64 electrodes. As a base state for the experiments, we chose a state with very weak coupling that was attained by adding individual external resistances to each of the electrodes and using a highly conductive electrolyte so that the potential drop in the electrolyte was very small relative to that in the external circuit.

Variations in surface properties occur on polycrystalline electrode surfaces, both for single large electrodes and for arrays of smaller electrodes. Thus, the rate of reaction and the dynamics of the individual elements vary somewhat. The currents of most of the individual electrodes exhibit low-dimensional chaotic behavior. A typical time series is shown in Figure 3a. The power spectrum (Figure 3b) has a dominant peak at f = 1.240 Hz, and the reconstructed attractor (Figure 3c) is low-dimensional ($D_1 = 2.3 \pm 0.1$). The dynamics of most of the other oscillators are similar. However, because of the surface heterogeneities in a typical experiment, the behaviors of 5−10 elements differ from that shown and exhibit either banded chaotic or noisy periodic behavior. (With added coupling, the number of banded or periodic elements decreases and eventually becomes zero; that is, with small coupling, all of the elements exhibit the dynamics shown in Figure 3a−c.) Because the experiment was designed so that the coupling strength was low, the elements in the array were not synchronized.[25] At any given time, the currents of the elements and the positions in state space differed. Thus, a snapshot of the 64 elements on the attractor (not shown) would yield points distributed over the attractor of Figure 3c. In a similar manner, as seen in Figure 3d, a stroboscopic plot of all 64 electrodes obtained using the mean frequency of the oscillators yields a distribution of points covering the attractor.

We see that, as a result of the very weak inherent coupling between the elements, the oscillators do not show synchronous behavior. The differences among the oscillators can be seen in the instantaneous phases and in the frequency distribution. In Figure 3e, the frequencies of the elements on the array are shown; the middle

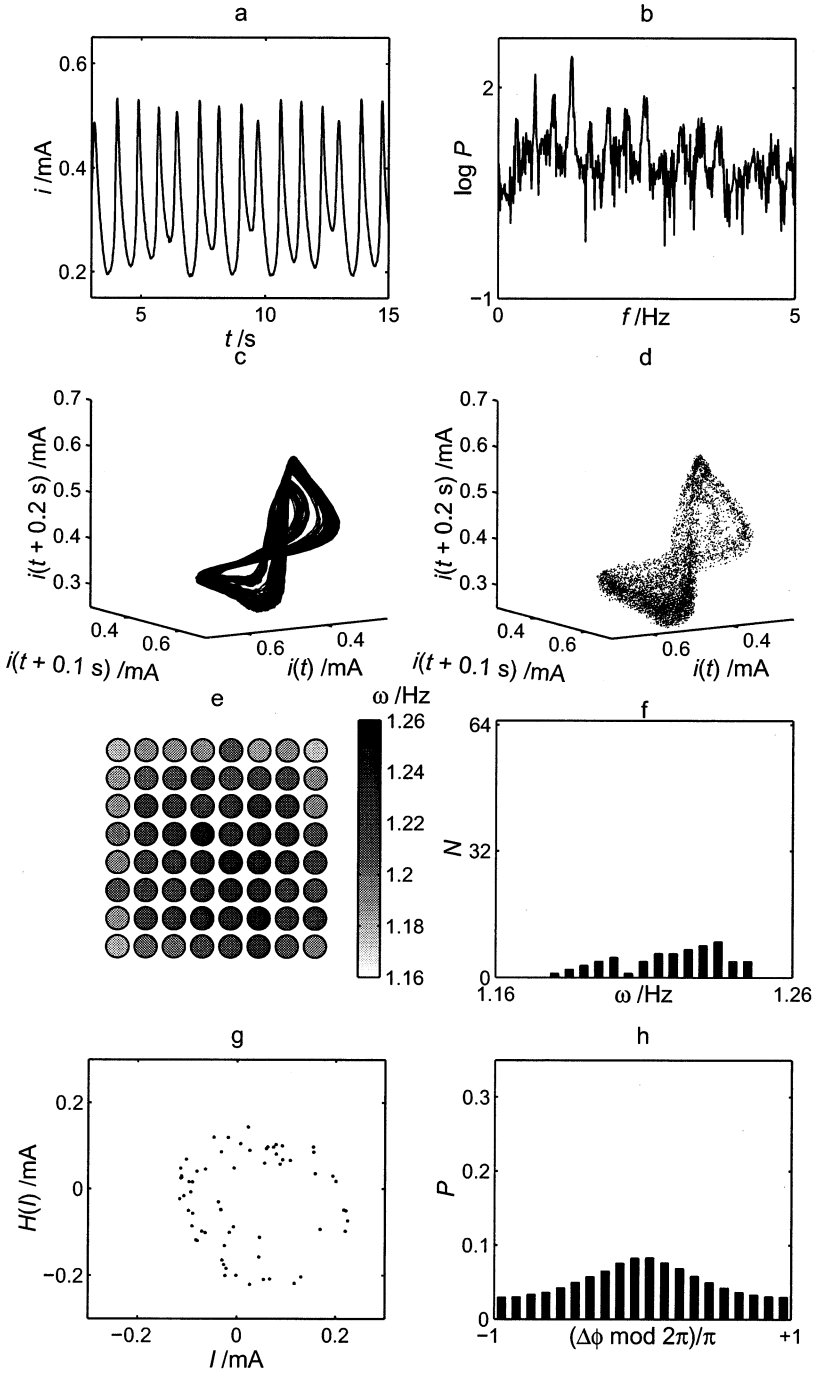

Figure 3. Dynamics of 64 electrodes without added coupling. (a) Representative time series of current of individual element. (b) Power spectrum of time series from individual element. (c) Reconstructed attractor from individual current using time delays. (d) Stroboscopic plot (using mean frequency, $\omega = 1.219$ Hz) of the phase points of the 64 elements. (e) Distribution of the frequencies of the oscillators on the array. (f) Histogram of the frequencies. (g) Phase portrait snapshot of the 64 oscillators. (h) Cyclic phase difference distribution of all pairs in the array.

sites have, on average, somewhat higher frequencies than the overall mean. The histogram of frequencies (Figure 3f) shows a rather flat distribution with a mean frequency of 1.219 Hz and a standard deviation of 18 mHz.

A snapshot of the phase portrait shows that the phase points are fairly uniformly distributed (Figure 3g). The cyclic phase differences ($\Delta\phi_{j,k}$ mod 2π, where $\Delta\phi_{j,k} = \phi_j - \phi_k$) have been calculated for all possible pairs in the array [there are $(64 \times 63)/2 = 2016$ such pairs], and the distribution is shown in Figure 3h. The distribution has a shallow maximum that is likely due to the very weak coupling through the electrolyte.

C. Effect of Weak Global Coupling on Individual Elements and Their Interactions. We now consider the addition of a weak global coupling, $\epsilon = 0.1$. With this added coupling, there is only a slight change in the qualitative dynamics of the individual elements. The time series of current for an individual element (Figure 4a), its power spectrum (Figure 4b, $f_{max} = 1.230$ Hz), and the reconstructed attractor (Figure 4c) and its dimension (2.3 ± 0.1) are similar to those in Figure 3, i.e., similar to those obtained without added coupling. As we shall see below, however, the collective behavior of the elements changes dramatically with the added coupling. These changes in the collective behavior are

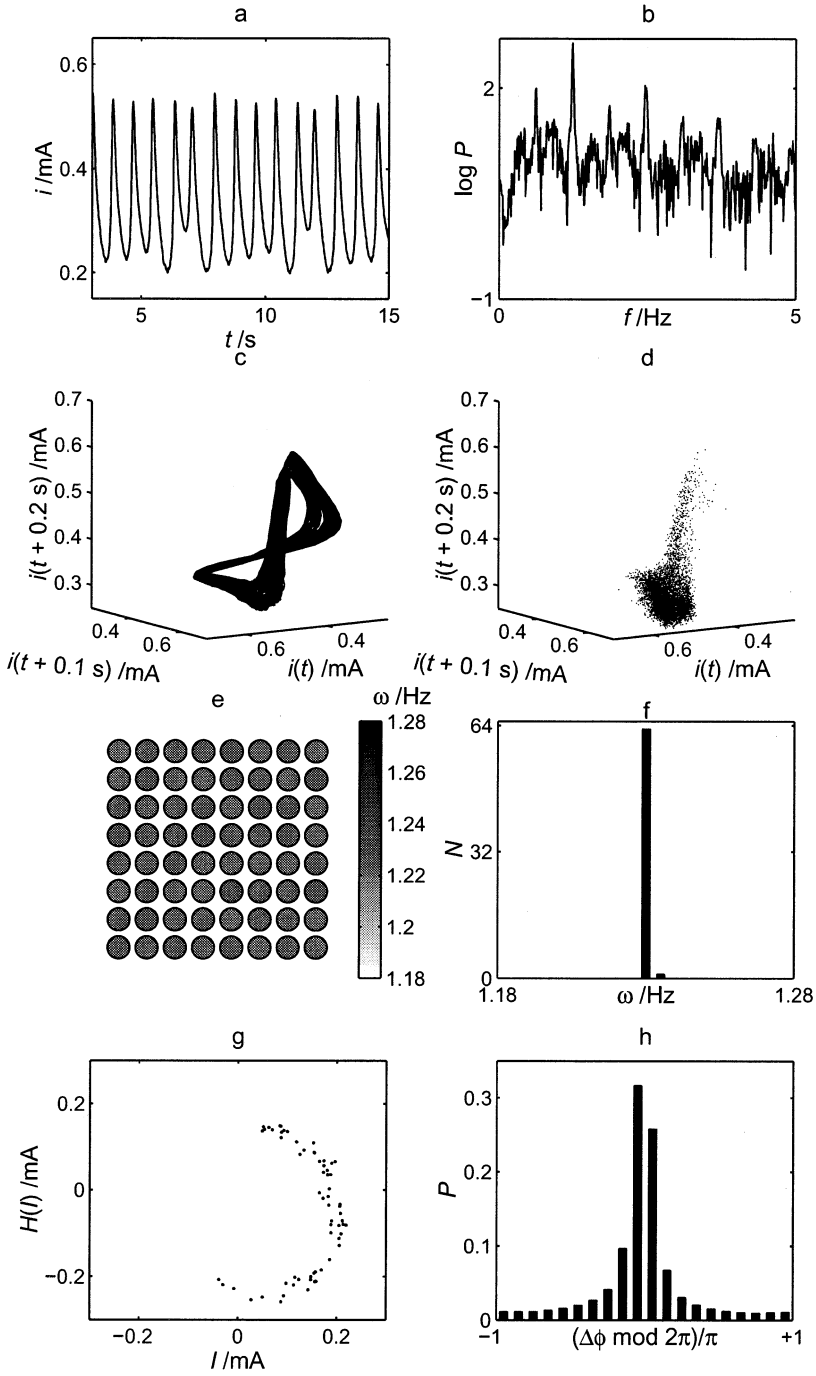

Figure 4. Dynamics of 64 electrodes with added global coupling ($\epsilon = 0.1$). (a) Representative time series of current of individual element. (b) Power spectrum of time series from individual element. (c) Reconstructed attractor from individual current using time delays. (d) Stroboscopic plot (using mean frequency, $\omega = 1.230$ Hz) of the phase points of the 64 elements. (e) Distribution of the frequencies of the oscillators on the array. (f) Histogram of the frequencies. (g) Phase portrait snapshot of the 64 oscillators. (h) Cyclic phase difference distribution of all pairs in the array.

associated with a phase synchronization of the individual elements. The added weak coupling narrows the frequency distribution of the elements. In the example shown here, the frequencies of 63 oscillators are the same (Figure 4e and f, $\omega = 1.230$ Hz) and that of the remaining element is 1.237 Hz. In some experiments at this coupling strength, all of the elements had the same frequency; in others, 1−3 elements differed. The phase points in the phase portrait (Figure 4g) are not as uniformly distributed as in Figure 3g; the points all lie on the right side of the figure. As a result, the cyclic phase difference distribution (Figure 4h) has a maximum around a phase difference of zero.

The results shown in Figure 4 clearly indicate a qualitative change in the phase dynamics as weak coupling is added to the system. Although the coupling is not strong enough to synchronize the elements, a weaker form of interaction, phase synchronization, has set in. The phase synchronization of these chaotic oscillators is similar to the phase locking of noisy periodic oscillators in which the phase differences are bounded but neither zero nor constant in time.[21] As a result of this phase synchronization, the phase points

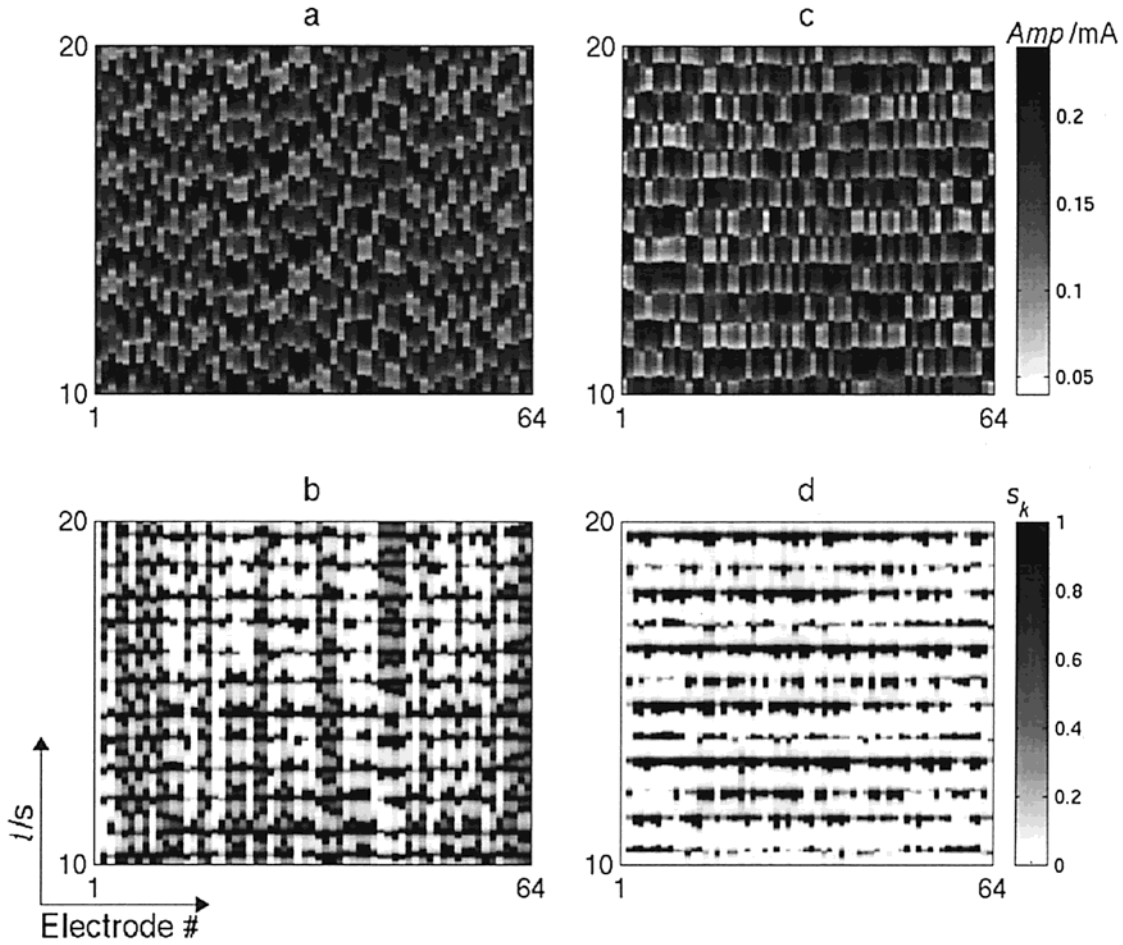

Figure 5. Gray-scale plot of the amplitudes (A) and phase differences (s_k) of the 64 oscillators without ($\epsilon = 0.0$) and with ($\epsilon = 0.1$) global coupling. (a) Amplitudes at $\epsilon = 0.0$. (b) Phase differences (s_k) at $\epsilon = 0.0$. (c) Amplitudes at $\epsilon = 0.1$. (d) Phase differences (s_k) at $\epsilon = 0.1$.

on the stroboscopic plot (Figure 4d) do not cover the entire attractor.

The onset of phase synchronization can also be seen in the gray-scale plots of amplitudes and phase differences of the 64 oscillators in Figure 5. A metric (s_k) for the phase differences is defined as

$$s_k = \sin^2\left(\frac{\phi_k - \phi_1}{2}\right), \quad k = 1, ..., N \tag{7}$$

At $\epsilon = 0$ (Figure 5a,b), both the amplitudes and the phase differences (s_k) have a disordered structure. At $\epsilon = 0.1$ (Figure 5c,d), the amplitudes exhibit less erratic behavior, and the phase differences are small, with occasional excursions close to the maximum of the time series of the oscillators.

D. Collective Behavior with Weak Global Coupling. In reaction systems, it is often the collective behavior, or the mean rate of reaction, that is important and sometimes the only variable that can be measured. In electrochemistry, such a quantity is the mean current

$$h(t) = \frac{1}{N}\sum_{k=1}^{N} i_k(t) \tag{8}$$

The mean currents as a function of time are shown in Figure 6 for three cases: without ($\epsilon = 0$), with small ($\epsilon = 0.1$), and with large ($\epsilon = 1$) added global coupling. Without added coupling (Figure 6a,b), the current time series shows small, irregular variations, and the corresponding attractor is of high complexity (Figure 6b). The power spectrum still has the largest peak at close to the average inherent frequencies, but its power is much reduced. At $\epsilon = 0.1$, the mean current exhibits (Figure 6c,d) periodic-like oscillations. The power spectrum has a large peak at around $f = 1.230$ Hz corresponding to the synchronized frequencies. The width of the peak is similar to that of an individual current, but strong superharmonics at multiples of the inherent frequencies can be observed. Small deviations from a limit-cycle behavior have also been found in numerical simulations and have been attributed to finite-size effects.[17] With a further increase in the coupling strength ($\epsilon > 0.1$), the regular periodic behavior of the mean current disappears, and the total current exhibits chaotic-like behavior similar to that of the individual elements. For comparison, we present in Figure 6e,f the behavior for $\epsilon = 1$, i.e., for a region of identical synchronization. Obviously, the time series of the mean current, its power spectrum, and the reconstructed attractor are similar to those obtained with a single, uncoupled electrode. The power spectrum in Figure 6e is broader, and the dominant peak has less power than that of the $\epsilon = 0.1$ case (Figure 6c). Note that, in all three cases shown in Figure 6, the individual oscillators are undergoing chaotic behavior.

A series of experiments was performed in which both the number of elements (N) and the coupling strengths were systematically varied to obtain statistical information on the mean current. In Figure 7a, the variance of the mean current is shown as a function of the number

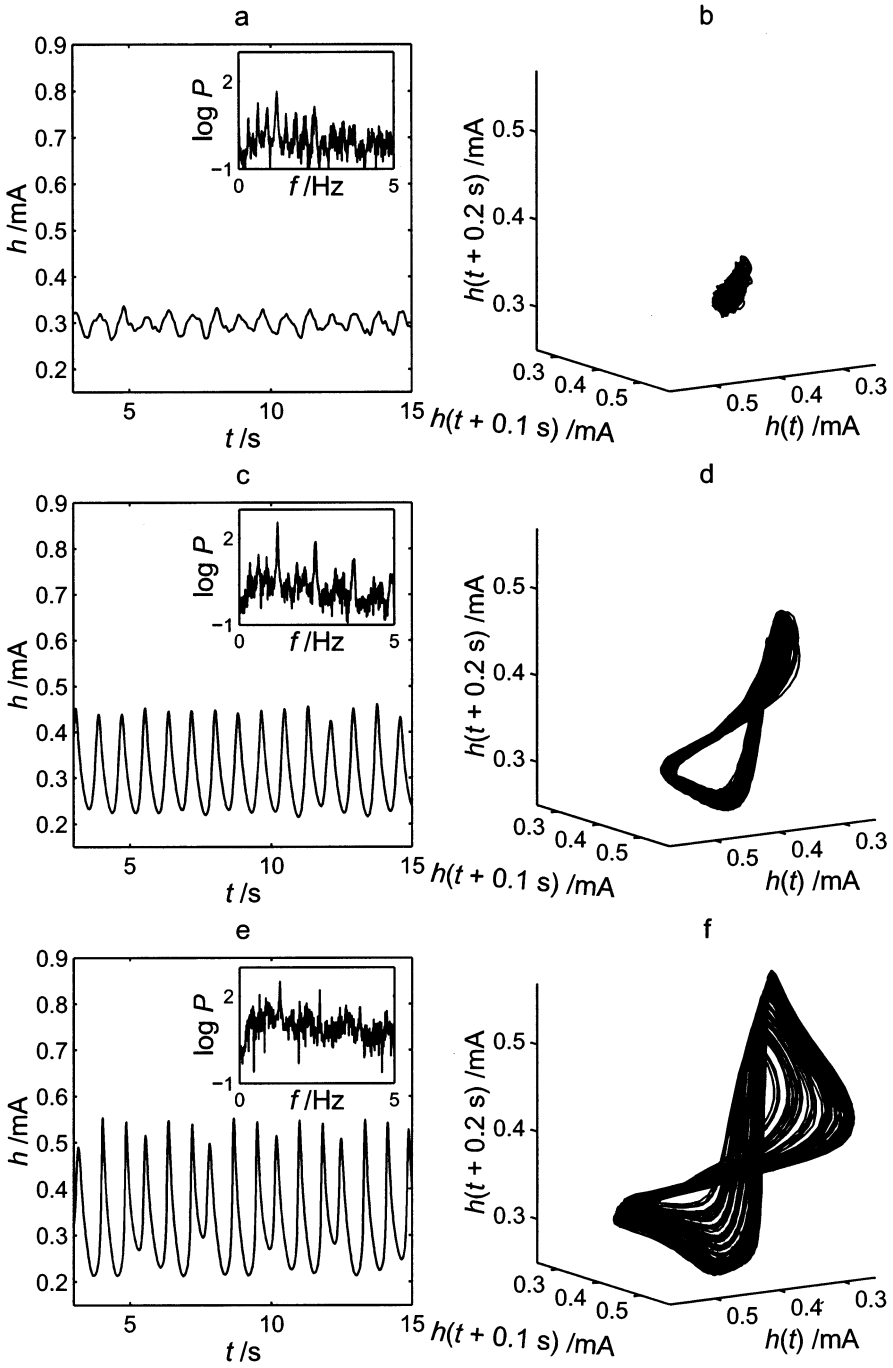

Figure 6. Dynamics of the collective behavior (mean current, h) of the 64 electrodes at different global coupling strengths. (a) Time series of mean current and its power spectrum (inset) without added coupling ($\epsilon = 0.0$). (b) Reconstructed attractor of the mean current using time delays at $\epsilon = 0.0$. (c) Time series of mean current and its power spectrum (inset) with weak global coupling ($\epsilon = 0.1$, phase synchronization). (d) Reconstructed attractor at $\epsilon = 0.1$. (e) Mean current and power spectrum (inset) with added strong global coupling ($\epsilon = 1.0$, identical synchronization). (f) Reconstructed attractor at $\epsilon = 1.0$.

of elements at different coupling strengths on a logarithmical plot. If there were no coherence among the elements of the array, the variance should follow the law of large numbers, i.e., it should depend on N as $1/N$. In our experiments, for $\epsilon = 0$, the variance of the mean current scales with $N^{-0.99}$, and therefore, the law of large number holds. Thus, as the number of elements increases, the magnitude of the temporal variations becomes smaller, and in the infinite-size limit, the variations would disappear. Adding weak global coupling ($\epsilon = 0.04$) has a dramatic effect on the scaling law: even for a small number of elements, there are deviations from a line of slope -1, and for $N \geq 36$, a saturation of the variance occurs. Such saturation has been observed in globally coupled chaotic maps.[13] At $\epsilon = 0.1$, the variance decreases only slightly with increasing N. For $\epsilon = 1$, identical synchronization, the variance is independent of N. Thus, we see that the addition of small amounts of coupling (up to $\epsilon = 0.1$, where phase synchronization occurs and where the mean current is almost periodic) has a significant effect but that further increases to the identically synchronized chaotic state ($\epsilon = 1$) have only small effects on the variance.

We characterize the extent of phase synchronization by the index $\sigma_{1,1} = 1 - S/S_{max}$,[32] where S is the Shannon entropy $S = -\sum_i p_i \ln p_i$ of the cyclic phase distribution and S_{max} is the maximal entropy. Very small (close to zero) values of $\sigma_{1,1}$ imply no phase synchronization, and

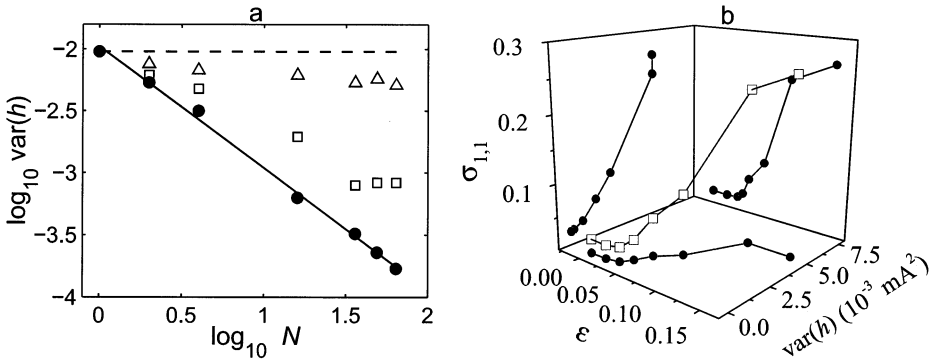

Figure 7. Dependence of variance of mean current [var(h)] on number of elements (N) and global coupling strength (ϵ). (a) Variance of the mean current [log var(h)] vs the number of elements at $\epsilon = 0$ (circles), 0.04 (squares), 0.1 (triangles), and 1.0 (dashed line). At $\epsilon = 0$, the linear fit gives a slope of -0.99. (b) Variance of the mean current and the synchronization index ($\sigma_{1,1}$) as a function of the coupling strength (ϵ) for $N = 64$.

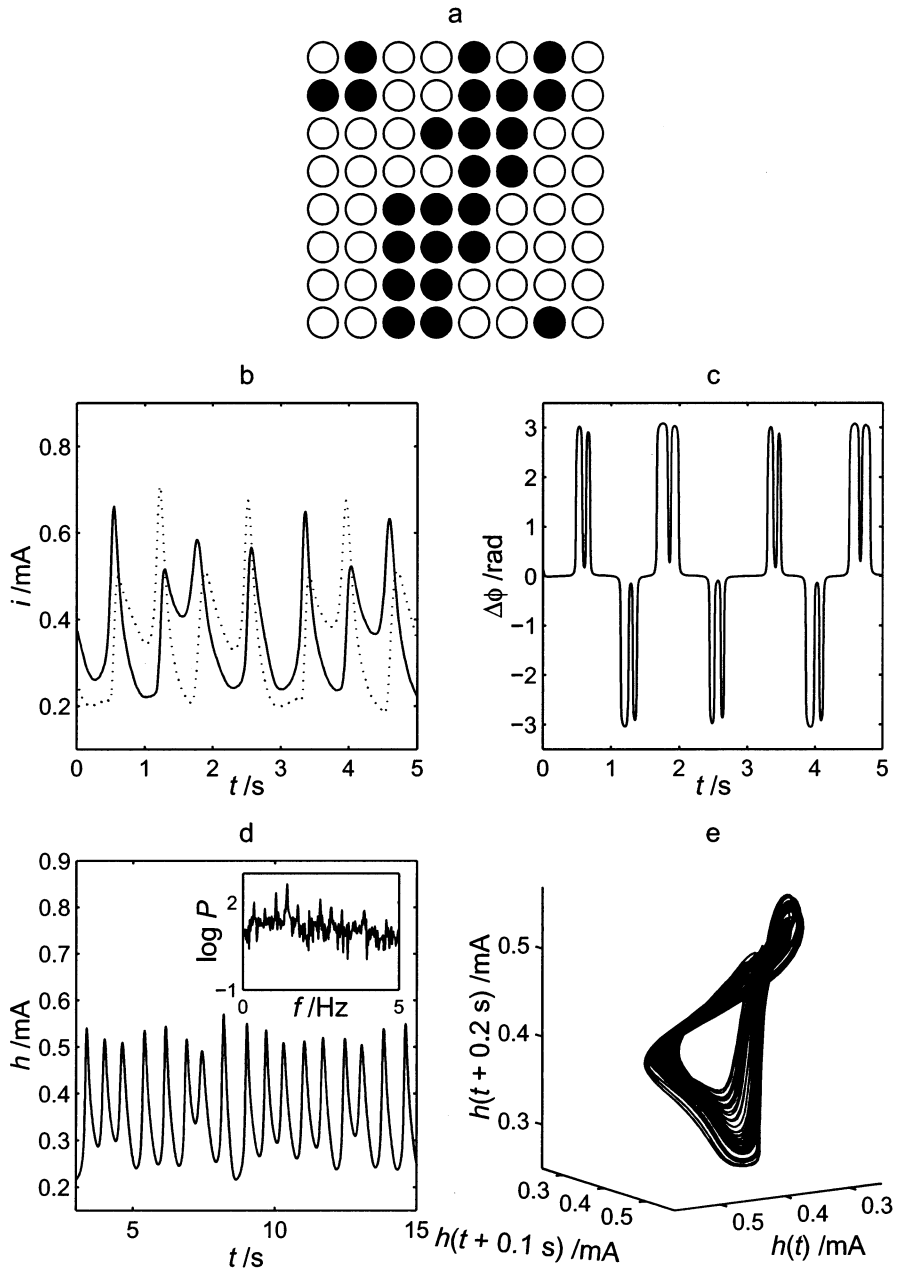

Figure 8. Dynamics of 64 electrodes with added global coupling ($\epsilon = 0.725$) in the cluster region. In the arrangement shown, the clusters contain 24 and 40 elements. (a) Arrangement of the elements in the two clusters. (b) Time series of the currents in each of the two clusters. Electrode 6 (solid line) is in the cluster of 40 elements; electrode 7 is the cluster of 24 elements. (c) Phase difference between the two clusters. (d) Time series and power spectrum (inset) of the mean current. (e) Reconstructed attractor of the mean current.

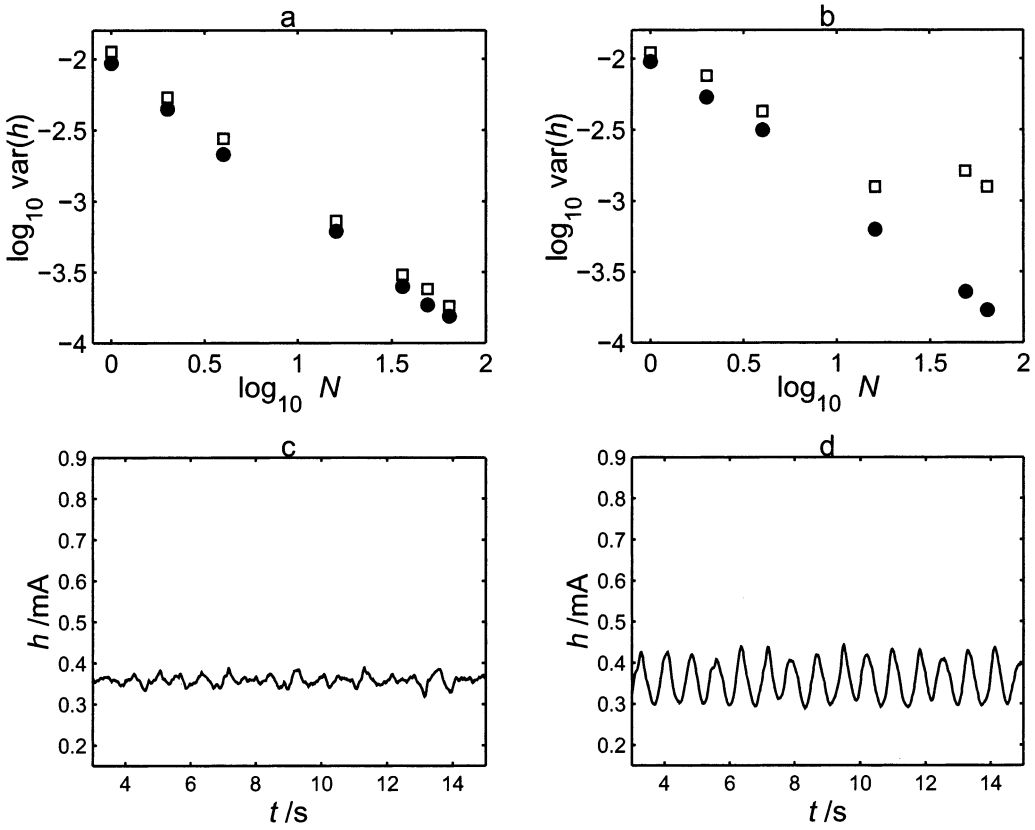

Figure 9. Dependence of mean current on stirring. (a) Variance of the mean current [log var(h)] vs the number of elements (N) without (circles) and with (squares) stirring on the array with 2 mm spacing. (b) Same as in a but with array spacing decreased to 1 mm. (c) Time series of mean current (h) on 64-electrode array of 2 mm spacing with stirring. (d) Time series of mean current (h) on 64-electrode array of 1 mm spacing with stirring.

a value of 1 corresponds to identical variation of phases. In our experiments, when $\sigma_{1,1}$ was larger than 0.15, the majority (>60) of the elements were phase-synchronized. In Figure 7b, the synchronization index $\sigma_{1,1}$ and the variance of the mean current [var(h)] are shown at different values of ϵ for the largest array ($N = 64$). With increasing global coupling strength from 0 to 0.15, both the variance of the mean current (bottom projection) and the synchronization index (right projection) increase in a sigmoidal way, and the two processes occur simultaneously.

E. Cluster Formation with Stronger Global Coupling. We have seen in the previous section that even weak global coupling produces phase synchronization of the elements. As the global coupling is made stronger, the elements remain phase-synchronized for all values of the parameter ϵ; in addition, other changes in the dynamics can occur. At higher values of ϵ, before the onset of identical synchronization, dynamical clustering is obtained.[25] Two stable chaotic clusters are seen; within a cluster, all of the elements have identical behavior except for small variations due to noise and system heterogeneities. [We say that two elements belong to a cluster if their separation distance in state space is less than some value (0.05 mA).] Although the elements within each cluster have identical chaotic dynamics, the dynamics in the two clusters differ. Both the number of elements in each of the two clusters and the configuration or arrangement of the elements within a cluster depend on the initial conditions. Representative configurations of cluster states with 40 and 24 elements in each cluster are shown in Figure 8a, and the time series of the clusters are shown in Figure 8b. Note that the dynamics of the two clusters are different from the dynamics of a single oscillator (Figure 2); for example, in Figure 8b, there are both larger and smaller oscillations. Because all elements in the array are phase-synchronized in this strongly coupled region, the two clusters are themselves phase-synchronized.

Because of the more complicated dynamics, there is no center of rotation, and thus, the use of the Hilbert phase is no longer possible. Therefore, the Gaussian phase[33,34] is calculated with the use of FFT filtering with a Gaussian filter function of mean frequency 1.415 Hz and standard deviation 8 Hz. The phase analysis shows that the two clusters are phase-synchronized with each other; they have the same frequency, and their phase differences are bounded. However, the phases are not simply delayed by some constant value; rather, they exhibit a more complicated dynamics. In Figure 8c, it is seen that the phase difference between the two clusters exhibits alternating positive and negative peaks separated by zero differences; this is caused by the alternating order of the maxima in the time series of the currents of the two clusters as seen in Figure 8b. Similar variations of the phase differences were observed for all cluster configurations. However, during the times at which the phase difference is close to zero, the amplitudes of the two clusters are not the same. The dynamics of their mean currents (Figure 8d,e) are more chaotic-like, similar to those in the identical synchronized region ($\epsilon = 1$). Furthermore, the amplitudes of the oscillations (the weighted means of the two clusters) are less than those of the two individual clusters but similar to that of the single oscillator (Figure 2).

F. Local Interactions through Stirring. We investigated the effect of weak coupling imposed by stirring. These experiments were done without added

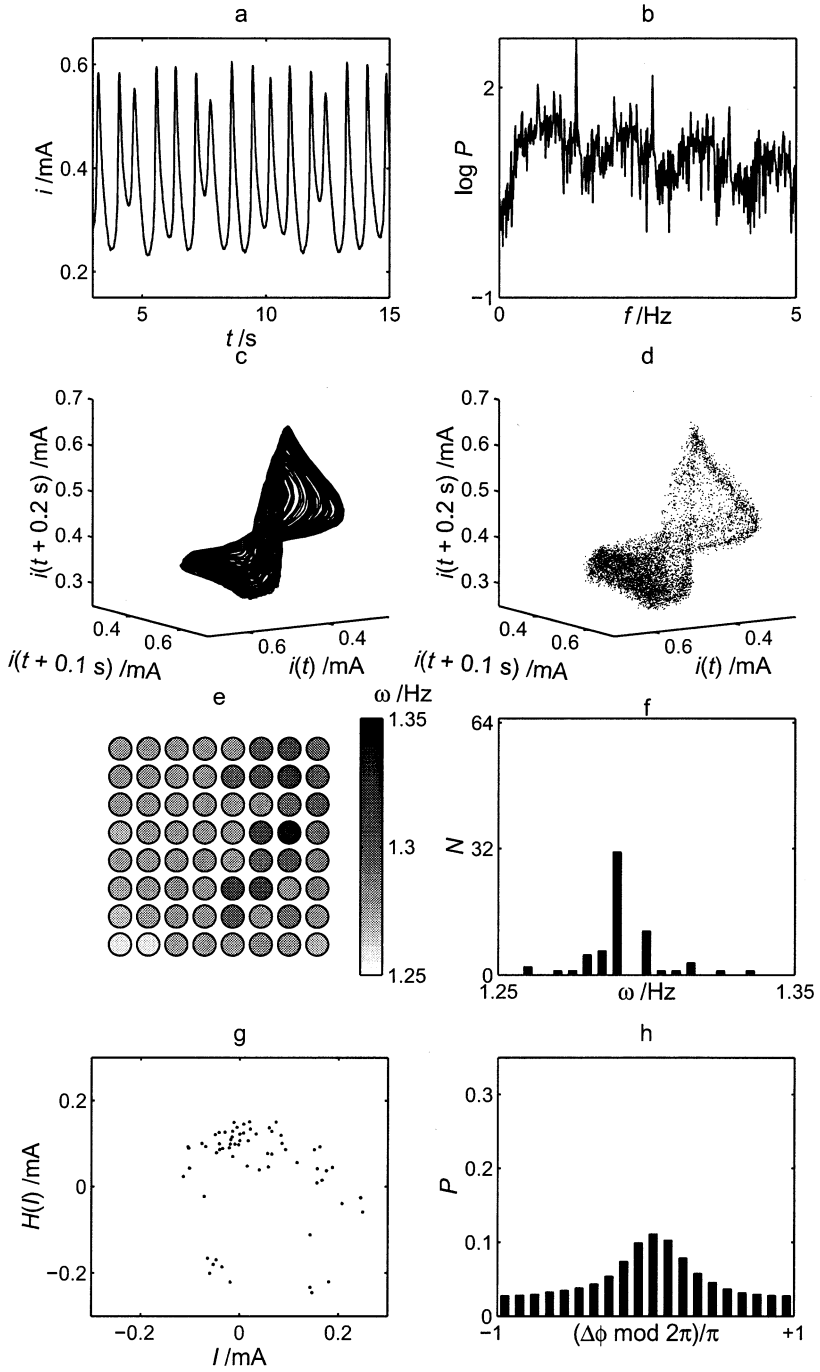

Figure 10. Dynamics of 64 electrodes (1 mm spacing) with stirring. (a) Representative time series of current of individual element. (b) Power spectrum of time series from individual element. (c) Reconstructed attractor from individual current using time delays. (d) Stroboscopic plot (using mean frequency $\omega = 1.291$ Hz) of the phase points of the 64 elements. (e) Distribution of the frequencies of the oscillators on the array. (f) Histogram of the frequencies. (g) Phase portrait snapshot of the 64 oscillators. (h) Cyclic phase difference distribution of all pairs in the array.

global coupling ($\epsilon = 0$) using two arrays with spacings among elements of 1 and 2 mm.

First consider the statistical features of the collective dynamics. The dependence of the variance of the mean current on system size is shown for the 2-mm-spacing array and the 1-mm-spacing array in Figure 9a,b, respectively. For the array with larger spacing, the law of large numbers is followed, and stirring has a minimal effect on the dynamics; the slope of the line is still approximately -1, but it is slightly above the value obtained without stirring. The behavior for the array with smaller spacing, however, is different, as seen in Figure 9b. Stirring increases the variance for all system sizes, and more significantly, there is saturation for systems of size $N \geq 16$. The time series for the mean current for the 2-mm-spacing array with stirring is presented in Figure 9c; it is similar to the result obtained without stirring, which is given for the 1-mm-spacing array in Figure 6a. For the array with smaller spacing, however, stirring increases coherence and results in macroscopic oscillations as seen in Figure 9d.

The stirring has an influence not only on the macroscopic behavior (for the closely spaced electrode) but also, to a lesser extent, on the degree of phase synchronization. The effects are not seen with the array of greater spacing. The individual dynamics with stirring

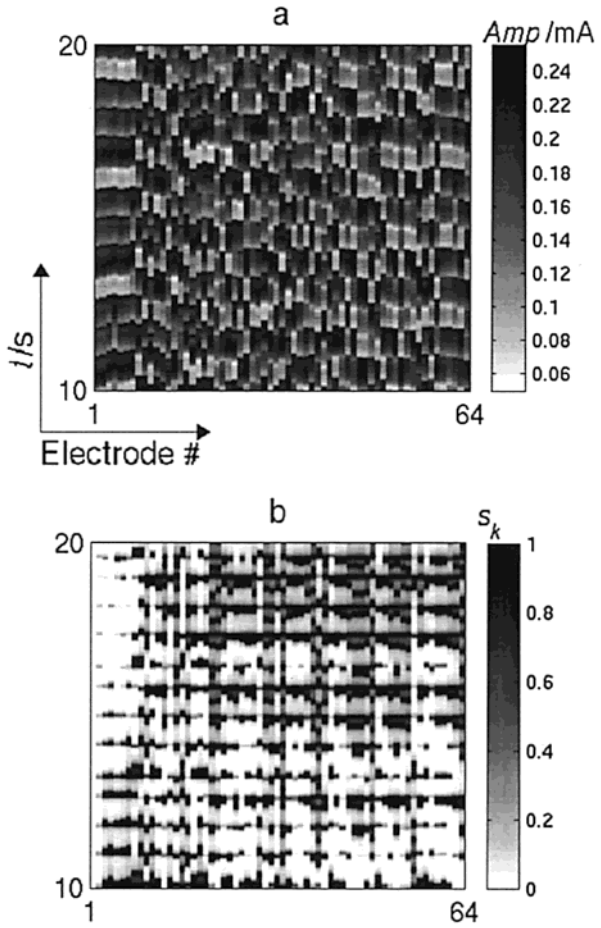

Figure 11. Dynamics of 64 electrodes (1 mm spacing) with stirring. (a) Gray-scale plot of the amplitudes of the individual currents. (b) Gray-scale plot of phase differences (s_k) of the elements.

for the 64-electrode array with smaller spacing are shown in Figures 10 and 11. The time series of the individual elements, their power spectra, and the attractors do not show significant differences from the results presented in Figure 3 that were obtained without stirring. The standard deviation of the frequencies decreased from 18 to 13 mHz with stirring, and the cyclic phase difference distribution showed a slightly larger maximum. The synchronization index increased from 0.022 to 0.043 with stirring; however, this value is still much smaller than that obtained with phase synchronization (0.15). The gray-scale plot of the amplitudes and the phases (Figure 11a,b) show a slightly more ordered behavior than in the uncoupled case, especially for certain regions of the electrode array; e.g., the first line of eight electrodes seems more synchronized than the others on both the amplitude and phase plots.

We thus see effects of stirring on the local dynamics and the collective behavior for the array with smaller spacing but not for the array with greater spacing. The space scale for the short-range coupling caused by the stirring is apparently in the range of 1−2 mm.

Discussion

We have presented results of experiments on the effects of weak coupling on the collective dynamics of a set of chaotically oscillating electrochemical reaction sites. As is usual in experimental systems, heterogeneities in the system produce slight differences in the properties of the individual elements; for example, the uncoupled oscillators have a distribution of frequencies. We investigate the effects of coupling on both the overall or mean reaction rate and the dynamics at the local positions.

Weak global coupling induced phase synchronization, where the frequencies of the oscillators became the same but identical synchronization of the elements did not yet occur. Along with the onset of phase synchronization, changes in the dynamics of the mean current occurred. Deviations from the law of large numbers were observed, i.e., the variance of the mean current did not decrease with increasing system size but rather reached a saturation value. Thus, in complex systems, the variation of averaged quantities cannot be made arbitrarily small with increasing system size because of inherent coherence. We see also that it is not always possible to infer even the qualitative behavior of local dynamics from global or mean measurements. For example, a periodic-like mean current is seen with weak coupling although the individual elements are chaotic. A complete description of such reaction systems would require high-frequency local measurements, which are often not available. Some indications of the extent of interactions can be obtained from analyses of the mean behavior; one indication of interaction and the effect on collective behavior is saturation of the variance of the mean rate with increasing system size.

The experiments also show a short-range coupling through the effect of stirring. The effects of stirring have not been as thoroughly explored in electrochemical systems—where coupling through the potential field often dominates[6]—as it has in other types of fluid/solid reaction systems. Although the coupling through transport imposed by stirring is very weak, its effect can be seen through the analysis of the collective oscillations, i.e., deviations from the law of large numbers, and, to a lesser extent, via an analysis of phase synchronization.

We have thus shown that very weak coupling in a chemically reacting system can lead to coherence and have a major effect on the overall rate of reaction, even though the effects on local dynamics are small. A characterization of such weak coupling can be obtained from a statistical analysis of macroscopic quantities.

Acknowledgment

We thank Bill Schowalter for his inspiration and guidance as a teacher and for his continued friendship in the subsequent years. This work was supported by the National Science Foundation (CTS-0000483) and the Office of Naval Research (N00014-01-1-0603).

Literature Cited

(1) Kuramoto, Y. *Chemical Oscillations, Waves and Turbulence*; Springer: Berlin, 1984.

(2) Lobban, L.; Luss, D. Spatial Temperature Oscillations during Hydrogen Oxidation on a Nickel Foil. *J. Phys. Chem.* **1989**, *93*, 6530.

(3) Mertens, F.; Imbihl, R.; Mikhailov, A. Breakdown of global coupling in oscillatory chemical reactions. *J. Chem. Phys.* **1993**, *99*, 8668.

(4) Slinko, M. M.; Ukharskii, A. A.; Jaeger, N. I. Global and nonlocal coupling in oscillating heterogeneous catalytic reactions: The oxidation of CO on zeolite supported palladium. *PCCP Phys. Chem. Chem. Phys.* **2001**, *3*, 1015.

(5) Middya, U.; Luss, D. Impact of global interactions on patterns in a simple system. *J. Chem. Phys.* **1994**, *100*, 6386.

(6) Krischer, K. In *Modern Aspects of Electrochemistry*; Conway, B. E., Bockris, O. M., White, R. E., Eds.; Kluwer Academic/Plenum Press: New York, 1999; Vol. 32, p 1.

(7) Mazouz, N.; Krischer, K.; Flätgen, G.; Ertl, G. Synchronization and pattern formation in electrochemical oscillators: Model calculations. *J. Phys. Chem. B* **1997**, *101*, 2403.

(8) Birzu, A.; Green, B. J.; Otterstedt, R. D.; Jaeger, N. I.; Hudson, J. L. Modelling of spatiotemporal patterns during metal electrodissolution in a cell with a point reference electrode. *PCCP Phys. Chem. Chem. Phys.* **2000**, *2*, 2715.

(9) Kiss, I. Z.; Wang, W.; Hudson, J. L. Experiments on arrays of globally coupled periodic electrochemical oscillators. *J. Phys. Chem. B* **1999**, *103*, 11433.

(10) Karantonis, A.; Shiomi, Y.; Nakabayashi, S. Coherence and coupling during oscillatory metal electrodissolution. *J. Electroanal. Chem.* **2000**, *493*, 57.

(11) Chaté, H.; Lemaitre, A.; Marcq, P.; Manneville, P. Nontrivial collective behavior in extensively chaotic dynamical systems: An update. *Physica A* **1996**, *224*, 447.

(12) Kaneko, K. Remarks on the mean-field dynamics of networks of chaotic elements. *Physica D* **1995**, *86*, 158.

(13) Kaneko, K. Globally coupled chaos violates the law of large numbers but not the central limit theorem. *Phys. Rev. Lett.* **1990**, *65*, 1391.

(14) Perez, G.; Pandolambruschini, C.; Sinha, S.; Cerdeira, H. A. Nonstatistical behavior of coupled optical systems. *Phys. Rev. A* **1992**, *45*, 5469.

(15) Perez, G.; Cerdeira, H. A. Instabilities and nonstatistical behavior in globally coupled systems. *Phys. Rev. A* **1992**, *46*, 7492.

(16) Pikovsky, A. S.; Kurths, J. Do globally coupled maps really violate the law of large numbers? *Phys. Rev. Lett.* **1994**, *72*, 1644.

(17) Brunnet, L.; Chaté, H.; Manneville, P. Long-range order with local chaos in lattices of diffusively coupled ODEs. *Physica D* **1994**, *78*, 141.

(18) Brunnet, L. G.; Chaté, H. Phase coherence in chaotic oscillatory media. *Physica A* **1998**, *257*, 347.

(19) Chaté, H.; Manneville, P. Emergence of effective low-dimensional dynamics in the macroscopic behavior of coupled map lattices. *Europhys. Lett.* **1992**, *17*, 291.

(20) Shibata, T.; Kaneko, K. Heterogeneity-induced order in globally coupled chaotic systems. *Europhys. Lett.* **1997**, *38*, 417.

(21) Rosenblum, M. G.; Pikovsky, A. S.; Kurths, J. Phase synchronization of chaotic oscillators. *Phys. Rev. Lett.* **1996**, *76*, 1804.

(22) Pikovsky, A. S.; Rosenblum, M. G.; Kurths, J. Synchronization in a population of globally coupled chaotic oscillators. *Europhys. Lett.* **1996**, *34*, 165.

(23) Sakaguchi, H. Phase transition in globally coupled Rössler oscillators. *Phys. Rev. E* **2000**, *61*, 7212.

(24) Kiss, I. Z.; Zhai, Y.; Hudson, J. L. Collective dynamics of chaotic chemical oscillators and the law of large numbers. *Phys. Rev. Lett.* **2002**, *88*, 238301.

(25) Wang, W.; Kiss, I. Z.; Hudson, J. L. Experiments on arrays of globally coupled chaotic electrochemical oscillators: Synchronization and clustering. *Chaos* **2000**, *10*, 248.

(26) Fei, Z.; Hudson, J. L. Chaotic Oscillations on Arrays of Iron Electrodes. *Ind. Eng. Chem. Res.* **1998**, *37*, 2172.

(27) Kiss, I. Z.; Wang, W.; Hudson, J. L. Populations of coupled electrochemical oscillators. *Chaos* **2002**, *12*, 252.

(28) Lev, O.; Wolffberg, A.; Sheintuch, M.; Pismen, L. M. Bifurcations to Periodic and Chaotic Motions in Anodic Nickel Dissolution. *Chem. Eng. Sci.* **1988**, *43*, 1339.

(29) Kiss, I. Z.; Wang, W.; Hudson, J. L. Complexity of globally coupled chaotic electrochemical oscillators. *PCCP Phys. Chem. Chem. Phys.* **2000**, *2*, 3847.

(30) Gábor, D. *J. Inst. Electron. Eng. Part 3* **1946**, *93*, 429.

(31) Pikovsky, A. S.; Rosenblum, M. G.; Osipov, G. V.; Kurths, J. Phase synchronization of chaotic oscillators by external driving. *Physica D* **1997**, *104*, 219.

(32) Tass, P.; Rosenblum, M. G.; Weule, J.; Kurths, J.; Pikovsky, A.; Volkmann, J.; Schnitzler, A.; Freund, H. J. Detection of n:m phase locking from noisy data: Application to magnetoencephalography. *Phys. Rev. Lett.* **1998**, *81*, 3291.

(33) DeShazer, D. J.; Breban, R.; Ott, E.; Roy, R. Detecting phase synchronization in a chaotic laser array. *Phys. Rev. Lett.* **2001**, *87*, 044101.

(34) Lachaux, J. P.; Rodriguez, E.; Van Quyen, M. L.; Lutz, A.; Martinerie, J.; Varela, F. J. Studying single trials of phase synchronous activity in the brain. *Int. J. Bifurcation Chaos* **2000**, *10*, 2429.

Received for review December 18, 2001
Revised manuscript received May 10, 2002
Accepted May 10, 2002

IE0110235